◆ Human Brain Mapping 29:1327–1342 (2008) ◆

Representation of UV-B-Induced Thermal and Mechanical Hyperalgesia in the Human Brain: A Functional MRI Study

Frank Seifert,[1] Isabella Jungfer,[2] Martin Schmelz,[3] and Christian Maihöfner[1,2]*

[1]*Department of Neurology, University of Erlangen-Nuremberg, Schwabachanlage 6, 91054 Erlangen, Germany*
[2]*Department of Experimental Physiology and Pathophysiology, University of Erlangen-Nuremberg, Universitätsstrasse 17, 91054 Erlangen, Germany*
[3]*Department of Anaesthesiology, Mannheim, University of Heidelberg, 68135 Mannheim, Germany*

Abstract: Surrogate models of pain and hyperalgesia allow the investigation of underlying mechanisms in healthy volunteers. Here, we investigated brain activation patterns during mechanical and heat hyperalgesia in an inflammatory human pain model using functional magnetic resonance imaging. Heat and mechanical hyperalgesia were induced on the right forearm by UV-B application in 14 healthy subjects. All four conditions (nonsensitized heat and nonsensitized mechanical pain, sensitized heat and sensitized mechanical pain) were perceptually matched. A 2 × 2 factorial analysis was performed. Areas with main effect of sensitization were insula, anterior cingulate cortex (ACC), prefrontal cortices (PFC), parietal association cortices (PA), thalamus, and basal ganglia. A main effect of modality with more activation during heat hyperalgesia was found in primary somatosensory cortex (S1), ACC, PFC, and PA. A main effect of modality with more activation during mechanical hyperalgesia was found in secondary somatosensory cortices, posterior insula, and contralateral inferior frontal cortex (IFC). An interaction of sensitization and modality was found bilaterally in IFC. Areas with similar effects of sensitization in both stimulus modalities were ACC, bilateral anterior insula and bilateral IFC. We conclude that different types of hyperalgesia in a human surrogate model of inflammatory pain produce different brain activation patterns. This is partly due to a differential processing of thermal and mechanical pain and an interaction of sensitization and modality in the caudal portion of the IFC. Finally, the data provide evidence for the existence of a common "sensitization network" consisting of ACC, bilateral anterior insula, and parts of the IFC. *Hum Brain Mapp 29:1327–1342, 2008.*

Key words: pain; hyperalgesia; fMRI; surrogate model; brain; somatosensory system

INTRODUCTION

Pain is a phenomenon with sensory-discriminative, motivational-affective, motor, and autonomic subdimensions. Over the last few years efforts have been made using functional imaging studies to encode brain processing of pain and to decipher the underlying neuronal network. This network, considered as the "neuronal matrix of pain" [Melzack, 1999], consists of primary (SI) and secondary (SII) somatosensory areas, insular cortices, anterior cingulate cortex (ACC), and prefrontal cortices (PFC). There is accumulating evidence that these

Both first authors contributed equally to this manuscript.

Contract grant sponsor: German Research Network on Neuropathic Pain (German Federal Ministry of Education and Research; BMBF).

*Correspondence to: Christian Maihöfner, Department of Neurology, University of Erlangen-Nuremberg, Schwabachanlage 6, D-91054 Erlangen, Germany.
E-mail: christian.maihoefner@uk-erlangen.de

Received for publication 26 February 2007; Revised 12 July 2007; Accepted 17 July 2007
DOI: 10.1002/hbm.20470
Published online 19 October 2007 in Wiley InterScience (www.interscience.wiley.com).

areas are linked to different aspects of the human pain sensation [Treede et al., 1999]. In general, a "lateral" (SI, SII, and posterior insula) and a "medial" (ACC, PFC, and anterior insula) pain system has been distinguished. The lateral system seems to predominantly encode the sensory discriminative component, whereas the medial system encodes the affective-motivational subdimension [Hofbauer et al., 2001; Maihofner and Handwerker, 2005; Maihofner et al., 2006b; Rainville et al., 1997; Treede et al., 1999].

Basically, pain can be nociceptive or neuropathic [Woolf and Mannion, 1999]. Nociceptive pain is a complex sensation preventing bodily harm and maintaining body integrity. If tissue damage takes place, a set of excitability changes in the peripheral and central nervous system may lead to pain hypersensitivity in the inflamed and surrounding tissue. In contrast, neuropathic pain is a pathological condition without biological advantage that causes suffering and distress [Jensen and Baron, 2003; Woolf and Mannion, 1999]. Such maladaptive pain typically results from damage to the nervous system. Both pain after tissue damage and neuropathic pain can be either spontaneous ongoing or stimulus evoked. During these conditions activity within the "neuromatrix of pain" can be increased or additional brain areas can be recruited [Apkarian et al., 2005]. Stimulus-evoked pathological pain sensations can be divided into allodynia or hyperalgesia [Ochoa and Yarnitsky, 1993]. Allodynia is a condition where normally innocuous stimuli evoke pain. Hyperalgesia means that painful stimuli are found to be more painful than normal. Different somatosensory submodalities can be involved in allodynia or hyperalgesia, e.g., touch, cold, or heat. Imaging studies have investigated surrogate models of evoked pain [Baron et al., 1999; Iadarola et al., 1998; Maihofner and Handwerker, 2005; Maihofner et al., 2003, 2004; Witting et al., 2001; Zambreanu et al., 2005] or patients with neuropathic pain [Ducreux et al., 2006; Hsieh et al., 1995; Maihofner et al., 2005, 2006a; Mailis-Gagnon et al., 2003; Petrovic et al., 1999; Peyron et al., 2004; Witting et al., 2006]; for a detailed review see Apkarian et al. [2005] and Tracey [2005]. However, often only one submodality of stimulus-evoked pain, e.g., mechanical or thermal, has been investigated or primary and secondary hyperalgesia have been compared [Maihofner and Handwerker, 2005]. Therefore, to compare brain activations of different submodalities of hyperalgesia, we induced both heat and mechanical hyperalgesia, using the UV-burn model [Bickel et al., 1998; Hoffmann and Schmelz, 1999] in healthy volunteers. The resulting areas of mechanical and heat hyperalgesia allowed us to compare the brain processing of both conditions directly and at balanced intensities. An advantage of the UV-B model is that the induced hyperalgesia is stable over long time and broadly follows the erythema response and does not extend beyond the irradiated area, so that at least by the use of small radiated areas the resulting hyperalgesia is highly localized to the area of inflammation [Harrison et al., 2004], although greater radiated areas are reported to induce relevant secondary hyperalgesia [Sycha et al., 2005].

METHODS

Subjects

A total of 14 healthy subjects [six males, eight females, mean age 25.14 ± 1.07 years) participated in the study. The volunteers were informed about the procedures of the study but were unaware of the specific experimental goals. Informed consent was obtained from all participants before the experiments and the study adhered to the tenets of the Declaration of Helsinki. The study was approved by the local ethics committee. All subjects were already experienced in psychophysical studies. The stimulation site was the middle aspect of the right volar forearm in all subjects.

Experimental Design

Our experimental design was a 2 × 2 factorial blocked design with the factors sensitization (hyperalgesia, no hyperalgesia) and modality (heat pain, mechanical pain).

Induction of Experimental UV-B-Induced Hyperalgesia

At least 8 weeks before the experimental session, the individual minimal erythema dose (MED) for UV-B irradiation was established at the right forearm using a calibrated UV source (290–320 nm, Saalmann multitester SBB LT 400, Saalmann Medizintechnik, Herford, Germany). For this purpose, five circular spots with a diameter of 1.5 cm at the ventral side of the left forearm were irradiated with increasing intensities of UV-B radiation (0.02–0.06 J/cm^2). One day prior to the experimental sessions, a skin area on the ventral side of the forearm was irradiated with UV-B receiving threefold of the individual MED. No spontaneous, ongoing pain was reported at the irradiated spots. As described previously [Bickel et al., 1998; Koppert et al., 2004], an erythema and mechanical and heat hyperalgesia developed within 24 h (see "Results" section), which were restricted to the irradiated area. Subjects were told to avoid additional sun or artificial UV exposure.

Psychophysical Testing

Psychophysical testing was performed outside the scanner on the day of the fMRI measurements previously to the scans and in the same subjects.

Thermal Simulation

Thermal stimuli were applied by a Peltier-driven thermotest device with a probe size of 30 × 30 mm^2 (TSA-II, NeuroSensoryAnalyzer, Medoc Advanced Medical Systems, Rimat Yishai, Israel) inside and 3 cm outside the UV-radiated area. The temperatures that were used ranged from 35 to 53.5°C. The temperature was increased stepwise for 0.5°C starting from a baseline temperature of 32°C. The time interval between each stimulus interval was 30 s. Pain ratings

were obtained using a numeric rating scale (NRS) ranging from 0 to 100. For fMRI measurement, only the temperature intensity, which was rated "40" on the NRS was used to measure brain activity during mechanical and heat pain and hyperalgesia at identical perceptual pain levels.

Mechanical Stimulation

Mechanical stimuli were delivered by a mechanical impact stimulator [Kohlloffel et al., 1991; Maihofner et al., 2006b] inside and 3 cm outside the UV-radiated area. Preliminary tests with a pin-prick stimulator revealed that secondary hyperalgesia does not exceed the erythema border more than 2 cm. Briefly, a pneumatically driven plastic projectile (weight 0.5 g; diameter 5 mm) guided by a 31-cm-long barrel provided painful impact stimuli on the subject's skin. With this device different pain intensities can be provoked according to the velocity of the projectile [Kohlloffel et al., 1991; Maihofner et al., 2006b]. Impact stimulation was applied in a block design with a frequency of 1 Hz. Each stimulation block lasted for 21 s, interrupted by a baseline of 21 s. Five stimulation blocks were applied over the course of the experiment. The following velocities were applied: 12, 16, 20, 24, 28, 32 m/s in ascending order. Again, pain ratings were obtained using an NRS ranging from 0 to 100. The NRS values were used to calculate stimulus-response functions. For fMRI measurement, only matched intensities of pain at NRS = 40 were used to measure brain activity during mechanical and heat pain and hyperalgesia at identical perceptual pain levels.

fMRI

Image Acquisition

Echoplanar images were collected on a 1.5 T MRI scanner (Sonata, Siemens Medical Solutions, Erlangen, Germany) using the standard head coil. For each subject, four time series (mechanical impact stimulation, heat stimulation, mechanical hyperalgesia, heat hyperalgesia) of 93 whole-brain images were obtained with a gradient-echo, echo-planar scanning sequence (EPI; TR 3 s, time to echo 40 ms, flip angle 90°; field of view 220 mm^2, acquisition matrix 64 × 64, 16 axial slices, slice thickness 4 mm, gap 1 mm). The first four images were discarded to account for spin saturation effects. A T1-weighted three-dimensional magnetization-prepared rapid acquisition gradient echo sequence (MPRAGE) scan (voxel size = 1.0 × 1.0 × 1.0 mm^3) was recorded in the same session as the functional measurements for the recording of the individual brain anatomy.

fMRI Study Design and MRI Sequence Order

MRI sequences were assessed in the following order: anatomical scout, MPRAGE, EPI in randomized order (i.e., heat stimulation, heat hyperalgesia, mechanical stimulation, mechanical hyperalgesia).

fMRI Data Analysis

Data analysis, registration, and visualization were performed with the fMRI software package BrainVoyager 2000, V4.9. (www.brainvoyager.com). Data were motion-corrected using sinc interpolation. Preprocessing furthermore included Gaussian spatial (FWHM = 4 mm) and temporal (FWHM = 3 volumes) smoothing of the functional data. Afterwards, the functional data were transformed into a standard stereotactic space and linear-interpolated to 3 × 3 × 3 mm^3 [Talairach and Tournoux, 1988]. A block design with two conditions (stimulus, baseline) was applied with each block lasting 21 s in which seven images were acquired. Each stimulation protocol served to obtain appropriate reference functions reflecting experimental and baseline conditions (stimulus = 1, baseline condition = 0). The stimulation protocols were convoluted with a canonical hemodynamic response function. The reference functions served as independent predictors for a general linear model. As implemented in the BrainVoyager software package, a *z*-transformation of the functional volume time courses for each subject was applied to take account of different baseline signal levels. Group analysis was performed resulting in *T*-statistical activation maps for the conditions heat hyperalgesia and mechanical hyperalgesia. Contrast comparisons were performed to test for differences between experimental conditions (heat hyperalgesia vs. perceptually matched heat pain on nonsensitized skin, mechanical hyperalgesia vs. perceptually matched mechanical pain on nonsensitized skin, heat hyperalgesia vs. mechanical hyperalgesia). The contrast comparison of heat pain vs. mechanical pain on nonsensitized skin was presented in a previous study [Maihofner et al., 2006b]. The 2 × 2 factorial design allowed us to separate brain areas with a main effect of sensitization, brain areas with a main effect of modality, brain areas with a main effect of both factors and brain areas with an interaction of sensitization and modality. For that purpose, the following contrasts were calculated: (i) effect of sensitization, averaged across both modalities, (ii) effect of modality, averaged across both sensitization states, and (iii) the interaction contrast of sensitization and modality. Those areas with a main effect of at least one the factors or with an interaction of both factors were analyzed further to delineate the nature of the main effects and interactions by means of the parameter estimates of all four conditions. Furthermore, a conjunction analysis was performed to delineate those areas with (i) similar effects of sensitization regardless of modality and (ii) similar effects of modality regardless of sensitization state. For all contrasts, corresponding *P*-values were corrected for multiple comparisons using Bonferroni correction over all voxels. Maps were thresholded at $P < 0.0005$ (activations during different conditions) and $P < 0.05$ (comparisons between different conditions) (uncorrected, two-tailed) as indicated and at a minimum cluster size of 300 mm^3. The cluster size criterion was used as a conservative measure to minimize false positive activations [Maihofner and Handwerker, 2005].

Statistical Analysis

The psychophysical data are presented as mean ± SEM. Statistical evaluation was performed using the STATISTICA software package. To assess statistically significant differences between pain thresholds the Wilcoxon matched pairs test was used. P values < 0.05 were considered to be statistically significant.

RESULTS

Psychophysics

Mean stimulus-response functions for heat pain, heat hyperalgesia, mechanical impact pain, and mechanical hyperalgesia are shown in Figure 1. The stimulus-response functions show a consistent increase in pain ratings to heat and mechanical stimulation with a significant leftward shift of the corresponding stimulus-response functions. The individual stimulus intensity (temperature or velocity) that induced a pain intensity rated as "40" on an NRS ranging from 0 to 100 was chosen for the fMRI experiment. The mean stimulus intensities to provoke a pain rating of "40" on the NRS for heat pain and heat hyperalgesia were (49.5 ± 0.53)°C and (45.25 ± 0.03)°C ($P < 0.005$, U-Test). The mean impact velocities to evoke this pain intensity were 24.86 ± 2.07 m/s and 21.0 ± 1.98 m/s (NS, U-Test, Wilcoxon Mached Pairs-Test), the mean cumulated ratings were 33.73 ± 2.68 and 45.27 ± 2.83 ($P < 0.005$, U-test) on an NRS ranging from 0 to 100 for mechanical impact pain and mechanical impact hyperalgesia. Thus, in both modalities significant hyperalgesia could be induced and pain intensity was matched in all four conditions.

Brain Activations During UV-B-Induced Heat- and Mechanical Hyperalgesia

The hypothesis of the present study was that the cerebral processing of heat and mechanical hyperalgesia might differ. Figure 2A,B shows the corresponding group activation maps for the conditions "heat hyperalgesia" (Fig. 2A) and "mechanical hyperalgesia" (Fig. 2B). Corresponding Talairach-coordinates, T-scores, Bonferroni-corrected P-values and cluster sizes are depicted in Table I. Axial brain slices are referred by their superior–inferior position relative to the AC-PC line. Prominent activations during heat hyperalgesia (Fig. 2A) were seen in contralateral S1 cortex (slices +45 to +55), contralateral M1 cortex (slices +35 to +55), bilateral S2 cortex (slices +20 to +35), bilateral parietal association cortex (PA) (slices +35 to +45), bilateral insular cortex (slices 0 to +10), bilateral ACC (slices +35 to +45), ipsilateral posterior cingulate cortex (PCC) (slice +35), bilateral PFC (SFC, MFC, IFC) (slices +10 to +25), and bilateral inferior parietal lobulus (IPL) (slices +35). During mechanical hyperalgesia (Fig. 2B) activations were seen in contralateral S1 cortex (slice +45), contralateral M1 cortex (slices +45 to +55), bilateral S2 cortex (slices +10 to +20), bilateral PA (slices +35 to +45), bilateral insular cortex (slices 0 to +10), bilateral cingulate cortex (ACC) (slices +35 to +45), bilateral PCC (slice +35), bilateral PFC (SFC, MFC, IFC) (slices 0 to +45), and bilateral IPL (slices +20).

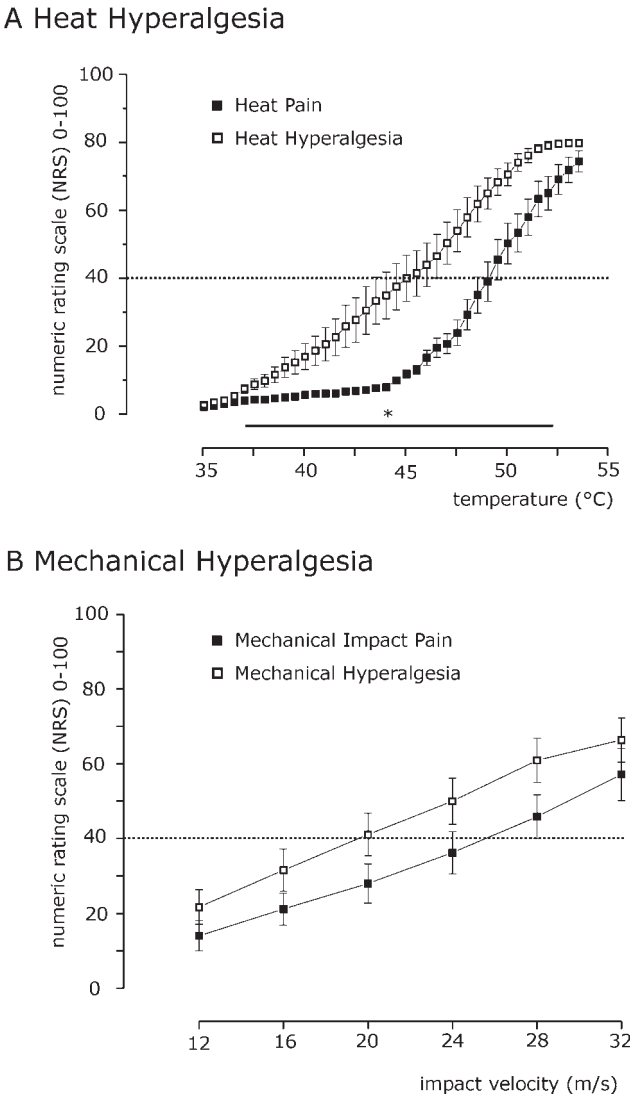

Figure 1.

Psychophysical testing. (**A**) Stimulus-response functions for heat pain inside and outside the area of UV-B application. The stimulus–response functions showed a consistent increase in pain ratings to heat stimulation with a leftward shift of the stimulus-response functions. The respective pain ratings were significantly higher inside the area of UV-B exposure. *Indicates $P < 0.05$, U-test. Means ± SEM. (**B**) Stimulus-response functions for mechanical impact pain inside and outside the area of UV-B application. The stimulus-response functions showed a consistent increase in pain ratings to mechanical impact-stimulation with a leftward shift of the stimulus-response function ($P < 0.005$ for the cumulated ratings, U-test). Means ± SEM.

TABLE I. Regions of cerebral activations

Region	Side	*X*	*Y*	*Z*	BA	*T*-score	*P*-value (corr.)	Cluster size (mm^3)
Heat hyperalgesia								
S1	Contralateral	−42	−36	49	3/40	4.403	0.000225	1,864
M1	Contralateral	−34	−23	52	4	5.175	0.000001	1,783
S2	Ipsilateral	52	−24	28	—	7.108	0.000001	7,375
S2	Contralateral	−51	−20	22	—	6.388	0.000001	3,584
Anterior insula	Ipsilateral	38	16	10	13	7.722	0.000001	11,522
Anterior insula	Contralateral	−34	18	9	13	7.410	0.000001	6,449
ACC	Ipsilateral	7	22	38	24/32	7.20	0.000001	3,817
ACC	Contralateral	−4	16	36	24/32	6.354	0.000001	2,209
SFC	Ipsilateral	21	46	38	8	6.801	0.000001	474
MFC/SFC	Ipsilateral	36	40	30	9	8.78	0.000001	10,121
MFC/SFC	Contralateral	−28	48	28	9	6.42	0.000001	2,353
IFC	Ipsilateral	51	10	11	44	6.11	0.000001	4,789
IFC	Contralateral	−48	4	8	44	5.87	0.000001	1,598
IPL	Ipsilateral	−54	−35	29	40	5.695	0.000001	925
IPL	Contralateral	−47	−36	31	40	6.819	0.000001	930
PA	Ipsilateral	42	−44	40	7/40	7.77	0.000001	12,225
PA	Contralateral	−39	−36	44	7/40	6.59	0.000001	10,501
TH	Ipsilateral	12	−11	13	—	6.85	0.000001	1,149
TH	Contralateral	−12	−12	7	—	5.55	0.000001	331
BG	Ipsilateral	18	10	9	—	8.452	0.000001	3,270
BG	Contralateral	−13	8	13	—	7.798	0.000001	4,218
Heat hyperalgesia vs. normal heat pain								
S1	Contralateral	−34	−40	55	3/40	2.993	0.002774	203
Anterior insula	Ipsilateral	38	1	9	13	3.657	0.000256	1,916
Anterior insula	Contralateral	−37	10	12	13	4.418	0.000010	3,652
ACC	Ipsilateral	1	16	35	24/32	3.070	0.002147	809
ACC	Contralateral	−3	14	35	24/32	3.561	0.000371	415
SFC	Ipsilateral	16	47	39	8	3.763	0.000169	1,102
MFC/SFC	Contralateral	−7	43	29	9	3.606	0.000313	653
MFC	Ipsilateral	37	36	25	10	3.595	0.000326	1,156
IFC	Ipsilateral	53	12	9	44	2.400	0.016438	2,042
PA	Ipsilateral	41	−46	43	7/40	3.152	0.001627	1,870
PA	Contralateral	−30	−47	49	7	3.419	0.000631	1,034
TH	Ipsilateral	11	−13	11	—	2.818	0.004842	288
Mechanical hyperalgesia								
S1/M1	Contralateral	−32	−19	53	3/4	7.774	0.000001	2,451
S2	Ipsilateral	52	−21	17	—	11.801	0.000001	11,895
S2	Contralateral	−47	−24	17	—	12.625	0.000001	14,939
Anterior insula	Ipsilateral	39	16	10	13	10.403	0.000001	13,699
Anterior insula	Contralateral	−37	15	11	13	9.600	0.000001	12,123
ACC	Ipsilateral	5	16	41	24/32	7.459	0.000001	1,246
ACC	Contralateral	−3	2	43	24/32	7.632	0.000001	3,077
MFC	Ipsilateral	37	39	24	9/10	9.080	0.000001	14,542
MFC	Contralateral	−31	44	25	9/10	6.643	0.000001	1,607
IFC	Ipsilateral	50	8	19	44	10.409	0.000001	6,800
IFC	Contralateral	−49	5	14	44	10.387	0.000001	3,662
IPL	Ipsilateral	52	−33	30	40	8.880	0.000001	4,863
IPL	Contralateral	−49	−34	27	40	9.482	0.000001	3,036
PA	Ipsilateral	45	−43	40	7/40	8.068	0.000001	8,981
PA	Contralateral	−46	−38	31	7/40	9.027	0.000001	4,341
TH	Ipsilateral	12	−8	15	—	8.715	0.000001	2,143
TH	Contralateral	−10	−13	13	—	7.567	0.000001	1,197
BG	Ipsilateral	15	8	12	—	8.170	0.000001	2,759
BG	Contralateral	−13	7	13	—	9.051	0.000001	3,604
Mechanical hyperalgesia vs. normal mechanical pain								
S1	Contralateral	−28	−37	57	1/2/3/5	3.240	0.001200	244
S2	Ipsilateral	41	−20	16	—	4.011	0.000061	2,244
S2	Contralateral	−49	−15	14	—	4.251	0.000021	4,003
Anterior insula	Ipsilateral	39	14	11	13	5.130	0.000001	12,416
Anterior insula	Contralateral	−32	13	10	13	5.189	0.000001	10,676
ACC	Ipsilateral	5	23	34	24/32	3.954	0.000077	2,414
ACC	Contralateral	−2	10	32	24/32	4.904	0.000001	1,486
MFC	Ipsilateral	32	38	32	9	3.815	0.000137	4,879

TABLE I. (continued)

Region	Side	*X*	*Y*	*Z*	BA	*T*-score	*P*-value (corr.)	Cluster size (mm^3)
MFC/SFC	Contralateral	−23	43	33	9	3.516	0.000440	1,191
IFC	Ipsilateral	49	13	8	44	4.270	0.000020	4,263
IFC	Contralateral	−45	12	10	44	4.121	0.000038	2,203
IPL	Ipsilateral	53	−40	32	40	3.381	0.000724	4,636
IPL	Contralateral	−48	−51	27	40	3.544	0.000397	2,254
PA	Ipsilateral	40	−50	38	7/40	3.637	0.000277	3,781
PA	Contralateral	−32	−52	25	39/40	3.709	0.000210	790
TH	Ipsilateral	12	−10	14	—	5.028	0.000001	3,681
TH	Contralateral	−10	−11	13	—	5.271	0.000001	4,573
PCC	Ipsilateral	1	−34	25	23	5.787	0.000001	3,128
PCC	Contralateral	−4	−35	28	23	4.252	0.000021	3,326
BG	Ipsilateral	16	13	11	—	3.911	0.000093	440
BG	Contralateral	−15	8	9	—	4.044	0.000053	750
Heat hyperalgesia vs. mechanical hyperalgesia								
Areas more activated during heat hyperalgesia								
S1	Contralateral	−41	−30	43	2/3/40/5	3.235	0.001222	4,783
ACC	Ipsilateral	3	28	32	24/32	2.425	0.015316	889
ACC	Contralateral	−3	31	32	24/32	2.707	0.006809	290
MFC/SFC	Ipsilateral	5	61	20	10	2.770	0.005619	1,219
SFC	Ipsilateral	15	40	51	8	3.047	0.002320	491
MFC/SFC	Contralateral	−32	54	18	9/10	2.645	0.008184	846
PA	Ipsilateral	39	−38	47	7/40	3.256	0.001135	1,991
PA	Contralateral	−28	−48	49	7	3.706	0.000212	4,557
Areas more activated during mechanical hyperalgesia								
S2	Ipsilateral	51	−20	15	—	7.228	0.000001	12,368
S2	Contralateral	−45	−24	16	—	7.284	0.000001	17,482
Insula	Ipsilateral	45	6	1	13	3.950	0.000079	620
Insula	Contralateral	−42	7	9	13/44	5.335	0.000001	4,759
IFC	Contralateral	−43	19	11	44/45	4.861	0.000001	2,730
IPL	Contralateral	−46	−35	23	40	5.606	0.000001	3,128
Main effect of sensitization averaged across both modalities								
PA	Ipsilateral	19	−63	42	7	3.718	0.000202	2,665
PA	Contralateral	−30	−44	47	7	3.472	0.000519	1,142
SFC/DLPFC	Ipsilateral	28	43	31	9	4.471	0.000008	5,027
SFC/DLPFC	Contralateral	−27	47	34	9	3.847	0.00012	598
ACC	Ipsilateral	3	17	36	24/32	3.954	0.000078	2,276
ACC	Contralateral	−3	13	36	24/32	4.8	0.000002	1,971
IFC	Ipsilateral	49	6	23	6/9/44	4.15	0.000034	5,661
IFC	Contralateral	−50	−1	16	6/9/44	5.085	0.000001	2,886
PCC	Ipsilateral	4	−23	32	23	3.652	0.000262	2,777
PCC	Contralateral	−2	−28	32	23	4.551	0.000005	3,292
Anterior insula	Ipsilateral	34	22	8	13	4.811	0.000002	5,390
Anterior insula	Contralateral	−34	22	8	13	4.787	0.000002	3,928
Posterior insula	Ipsilateral	36	−17	15	13	3.133	0.001736	1,023
Posterior insula	Contralateral	−40	−12	11	13	3.903	0.000096	1,304
BG	Ipsilateral	12	2	12	—	4.501	0.000007	2,262
BG	Contralateral	−12	6	13	—	4.863	0.000001	4,470
Thalamus	Ipsilateral	9	−17	10	—	4.411	0.000010	1,866
Thalamus	Contralateral	−9	15	11	—	5.158	0.000001	2,232
Main effect of modality averaged across both sensitization states								
Areas more activated during heat stimulation								
SI	Contralateral	−35	−32	55	3	2.189	0.0285	694
PA	Ipsilateral	16	−66	43	7	2.853	0.004345	4,018
PA	Contralateral	−25	−54	51	7	2.467	0.0136	2,596
SFC/DLPFC	Ipsilateral	28	50	34	9	3.239	0.001204	475
SFC/DLPFC	Contralateral	−24	47	32	9	3.45	0.000563	1,863
ACC	Contralateral	−3	15	35	32	2.116	0.00006	1,964
Areas more activated during mechanical stimulation								
S2	Ipsilateral	55	−23	14	—	7.673	0.000001	5,130
S2	Contralateral	−50	−34	16	—	7.757	0.000001	4,937
Posterior insula	Ipsilateral	43	−10	13	13	5.429	0.000001	1,672
Posterior insula	Contralateral	−38	−10	13	13	6.457	0.000001	4,933
IFC	Contralateral	−53	−3	21	6/9/44	4.599	0.000004	1,564

TABLE I. (continued)

Region	Side	*X*	*Y*	*Z*	BA	*T*-score	*P*-value (corr.)	Cluster size (mm^3)
Interaction of sensitization and modality								
Caudal IFC/PCG	Ipsilateral	44	3	9	44	3.332	0.00001	752
Caudal IFC/PCG	Contralateral	−49	7	8	44	2.87	0.0040	596
Conjunction analysis: areas with similar effect of sensitization during both modalities								
ACC	Ipsilateral	2	14	38	24/32			829
ACC	Contralateral	−1	14	37	24/32			490
Anterior insula	Ipsilateral	39	22	7	13			2,026
Anterior insula	Contralateral	−34	15	12	13			1,605
IFC	Ipsilateral	51	13	8	44			1,972
IFC	Contralateral	−50	12	11	44			905
Conjunction analysis: areas with similar effect of modality during both sensitization states								
Heat stimulation								
S1	Contralateral	−33	−35	48	3			4,035
PA	Ipsilateral	15	−72	41	7			742
PA	Contralateral	−15	−67	44	7			797
Mechanical stimulation								
S2	Ipsilateral	57	−21	13	—			4,251
S2	Contralateral	−50	−29	15	—			5,826
Posterior insula	Ipsilateral	44	−15	11	13			1,463
Posterior insula	Contralateral	−38	−21	14	13			4,914

S1, primary somatosensory cortex; M1, primary motor cortex; S2, secondary somatosensory cortex; PA, parietal association cortex; IPL, inferior parietal lobule; SFC, superior frontal cortex; MFC, middle frontal cortex; IFC, inferior frontal cortex; DLPFC, dorsolateral prefrontal cortex; ACC, anterior cingulate cortex; PCC, posterior cingulate cortex; PCG, precentral gyrus; TH, Thalamus; BG, basal ganglia. *P*-values are corrected for serial correlations.

Furthermore, during both conditions strong activations of bilateral basal ganglia (slices 0 to + 20) and thalamus (slices + 10) were observed.

Calculation of *T*-statistic Contrast Maps

To further compare cerebral activations during both types of hyperalgesia in more detail, we calculated three contrast maps. Corresponding Talairach-coordinates, *T*-scores, Bonferroni-corrected *P* values and cluster sizes of significantly different activated brain regions are depicted in detail in Table I. In a first statistical map, we compared brain activations during heat hyperalgesia vs. heat stimulation on normal skin (Fig. 2C). Significantly increased activations during heat hyperalgesia were found in bilateral insular cortices (slices 0 to +10), bilateral PA (slice +45), bilateral ACC (slice +35), bilateral PCC (slice +35), and bilateral PFC (SFC, MFC) (slices +10 and +35).

In a second statistical map, we compared brain activations during mechanical hyperalgesia with those during mechanical stimulation on normal skin (Fig. 2D). Significantly increased activations during the hyperalgesic pain were found in contralateral S1 cortex (slice +45), contralateral M1 cortex (slices +45 to +55), bilateral S2 cortex (slice +10), bilateral PA (slices +35 to +45), bilateral insula cortex (slices 0 to +10), bilateral cingulate cortex (ACC) (slices +35 to +45), bilateral PCC (slice +35), bilateral PFC (SFC, MFC, IFC) (slices 0 to +45), and bilateral IPL (slices +20).

A third statistical map was calculated by comparing brain activations during heat hyperalgesia with those of mechanical hyperalgesia (Fig. 3). Heat hyperalgesia (coded in red/yellow) activated to a significant greater extent bilateral PFC (SFC, MFC) (slices +20 to +55), bilateral anterior cingulate gyrus (ACC) (slice +35), contralateral PCC (slice +35), and PA (slices +35 to +55). In contrast, mechanical hyperalgesia (coded in blue/green) led to significantly more BOLD increase in bilateral S2 cortex (slices +10 to +20), and posterior insular cortex (slices 0 to +10).

Calculation of Factor Main Effects and Interactions

Two other contrast maps with the main effects of the two factors—sensitization and modality—were calculated. Areas with a main effect of sensitization are depicted in Figure 4A. Significantly increased activations during hyperalgesia, averaged across both modalities, were found in bilateral PFC (SFC, MFC, IFC; slices +20 to +55), with most prominent increases in bilateral dorsolateral prefrontal cortex (DLPFC; slice +35), bilateral posterior anterior cingulate gyrus (pACC; slice +35), bilateral anterior insula cortex (slices 0 to +10), bilateral posterior insula cortex (slices 0 to +10), bilateral PCC (slice +35), bilateral bilateral thalamus (slice +10), bilateral basal ganglia (slice +10), and bilateral PA (slices +35 to +55).

Areas with a main effect of modality (those more activated by heat stimuli are coded in red/yellow, those more activated by mechanical stimuli are coded in blue/green) are depicted in Figure 4B. Areas significantly more activated during heat stimuli compared with mechanical stimuli, averaged across both sensitization states, are the contralateral primary somatosensory cortex (S1), the bilateral PFC (SFC, MFC, IFC; slices +20 to +55), with most prominent activity increases in DLPFC (slice +35), and the bilateral PA (slices +35 to +45). Areas with significant greater

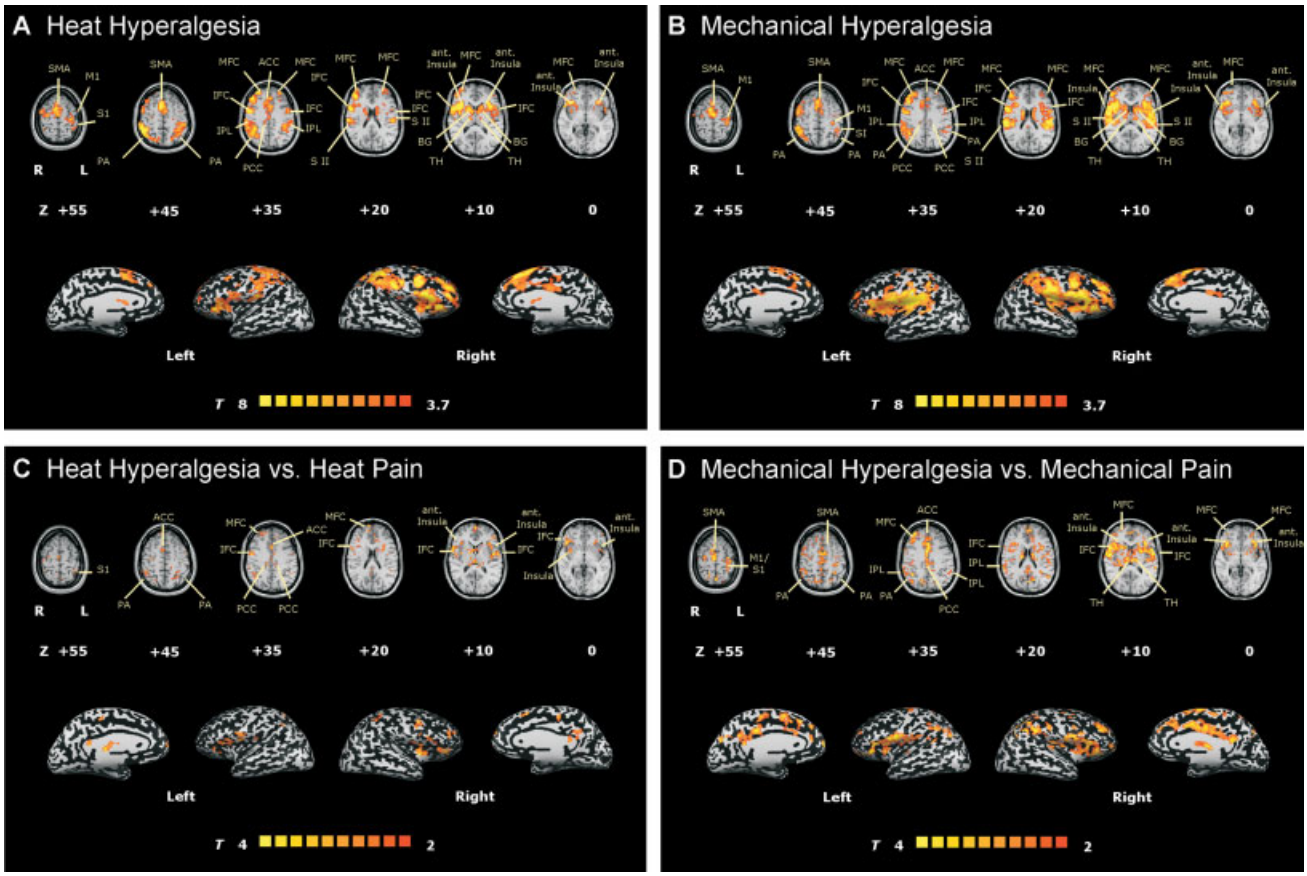

Figure 2.

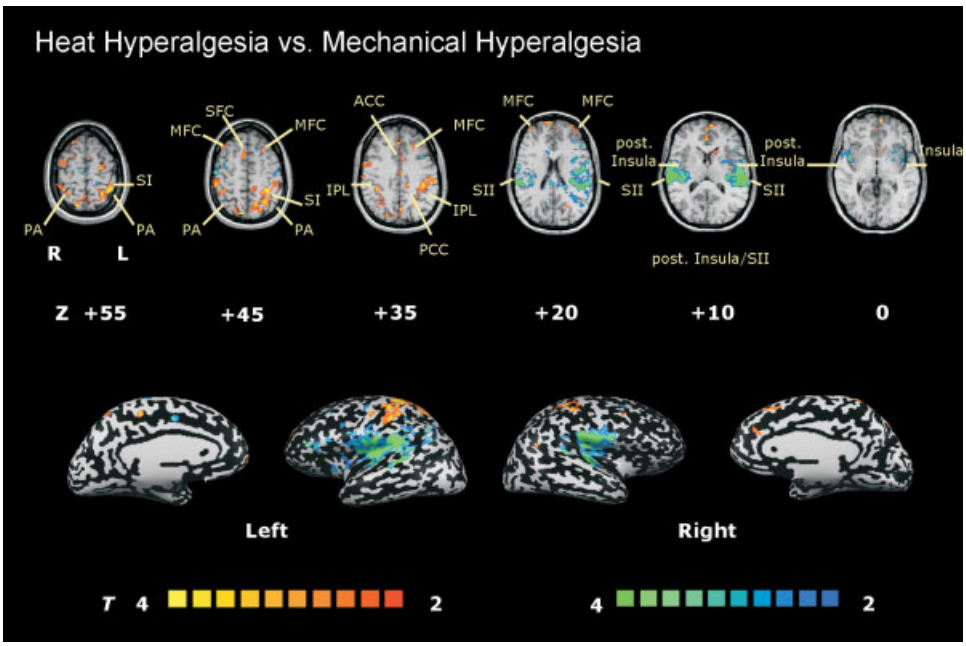

Figure 3.

activation during mechanical stimuli compared with heat stimuli, averaged across both sensitization states, were the bilateral secondary somatosensory cortex (S2; slices +10 to +20), bilateral posterior insular cortex (slices 0 to +10), and contralateral IFC (slice +20).

To address the hypothesis of our study, we calculated an interaction contrast of sensitization and modality. Significant sensitization–modality interaction was found bilaterally in the caudal portion of the inferior frontal cortex (IFC; Fig. 5).

Calculation of Conjunction Contrasts

A first conjunction contrast analysis revealed those areas with a similar effect of sensitization irrespective of modality (Fig. 6A). This network consists of the bilateral posterior ACC (slice +35), the bilateral insula cortex (slice 0 and +10), and the bilateral IFC (slice +10). A second conjunction contrast (Fig. 6B) revealed a common activation pattern for heat stimuli irrespective of sensitization state in contralateral S1 cortex (slice +45 and +55) and bilateral PA (slices +45 to +55); and for mechanical stimuli irrespective of sensitization state in bilateral secondary somatosensory cortex (S2) (slices +10 to +20), bilateral posterior insular cortex (slices 0 to +10).

DISCUSSION

In the present fMRI study we show that different types of UV-B-induced hyperalgesia, i.e., heat and mechanical hyperalgesia, result in different patterns of brain activation even when pain intensities were perceptually matched. Stronger activations in secondary somatosensory cortex (S2) and posterior insular cortex during mechanical hyperalgesia and increased PFC and PA activations during heat hyperalgesia suggest that different central pathways are involved in different types of hyperalgesia. Factor analysis revealed that the basis of the differences is both a differential processing of thermal and mechanical pain, and an interaction of sensitization and modality in the caudal portion of the IFC.

Basically, irradiation with UV-B causes a release of inflammatory mediators, such as prostaglandins, histamine, bradykinin, and serotonin. After exposure to inflammatory amounts of UV radiation, polymodal nociceptors develop spontaneous activity [Urban et al., 1993] and increased responses to noxious heat [Szolcsanyi, 1987]. Heat hyperalgesia is a peripheral mechanism induced by sensitization of c-nociceptors [Schmelz et al., 2003; Schmidt et al., 1995]. In contrast, mechanical impact hyperalgesia of the UV-B model is likely to result from both peripheral and central sensitization [Klein et al., 2005]. Central sensitization is induced by c-fiber discharge, but mediated by A-fibers [Ziegler et al., 1999]. This study was performed to answer the question whether the two types of hyperalgesia are processed differentially or if there is a "common hyperalgesia network".

A Common "Sensitization Network" Consisting of ACC, Anterior Insula, and Frontal Cortices

A significant sensitization-induced increase in activation was found in both modalities in a widespread network of cortical and subcortical brain regions: the ACC, anterior and posterior insula, prefrontal cotices (SFC, MFC, IFC), PCC, PA, basal ganglia, and thalamus. These areas are consistent with those previously reported to be involved in processing of painful stimuli in the hyperalgesic state

Figure 2.

Regions of cerebral activations related to the hyperalgesia conditions: (**A**) heat hyperalgesia and (**B**) mechanical hyperalgesia. Group activations were registered onto a Talairach-transformed brain in axial view, thresholded at $T > 4$, $P < 0.0005$, uncorrected for multiple comparisons and a cluster threshold of 300 voxels. For statistical comparison *T*-statistic contrast maps comparing (**C**) heat hyperalgesia vs. heat pain and (**D**) mechanical hyperalgesia vs. mechanical pain are depicted. The group statistic contrast maps are registered onto a Talairach-transformed brain, thresholded at $T > 2$, $P < 0.05$ uncorrected for multiple comparisons and a cluster threshold of 300 voxels. Activations seen in the left hemisphere are contralateral to the stimulation side. The Talairach-coordinates, *T*-scores, Bonferroni-corrected *P* values and cluster sizes are depicted in Table I. Abbreviations: ACC, anterior cingulate cortex; PCC, posterior cingulate cortex, TH, thalamus; SFC, superior frontal cortex; MFC, middle frontal cortex; IFC, inferior frontal cortex, S1, primary somatosensory cortex; S2, secondary somatosensory cortex; PA, parietal association cortex.

Figure 3.

The *T*-statistic contrast map compares the conditions "heat hyperalgesia" vs. "mechanical hyperalgesia". Areas activated more during heat hyperalgesia are coded in red/yellow, those more activated by mechanical hyperalgesia are coded in blue/green. The group statistic contrast maps are registered onto a Talairach-transformed brain, thresholded at $T > 2$, $P < 0.05$ uncorrected for multiple comparisons and a cluster threshold of 300 voxels. Activations seen in the left hemisphere are contralateral to the stimulation side. The Talairach-coordinates, *T*-scores, Bonferroni-corrected *P* values and cluster sizes are depicted in Table I. Abbreviations: ACC, anterior cingulate cortex; PCC, posterior cingulate cortex; TH, thalamus; SFC, superior frontal cortex; MFC, middle frontal cortex; IFC, inferior frontal cortex; S1, primary somatosensory cortex; S2, secondary somatosensory cortex; PA, parietal association cortex; IPL, inferior parietal lobule.

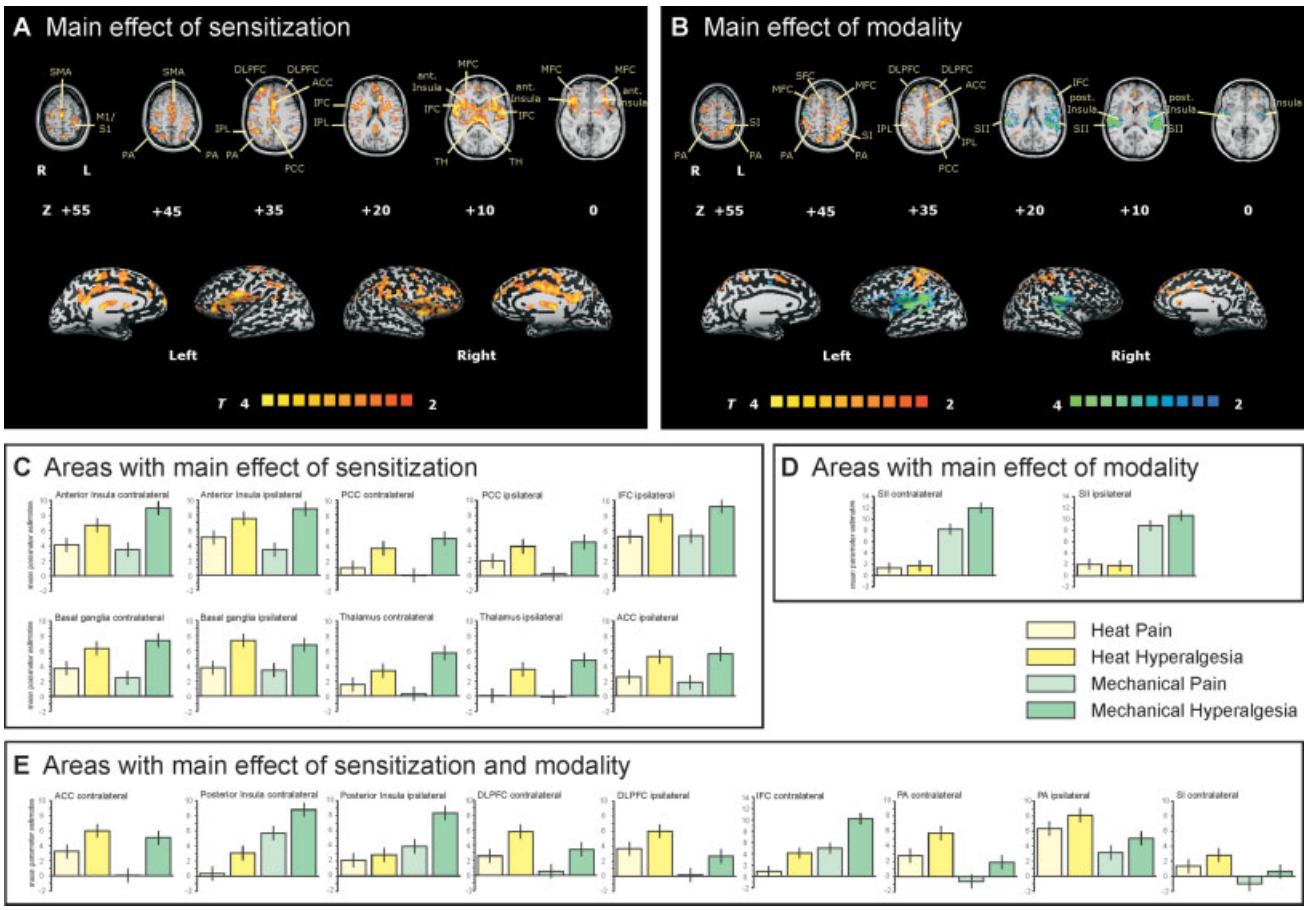

Figure 4.

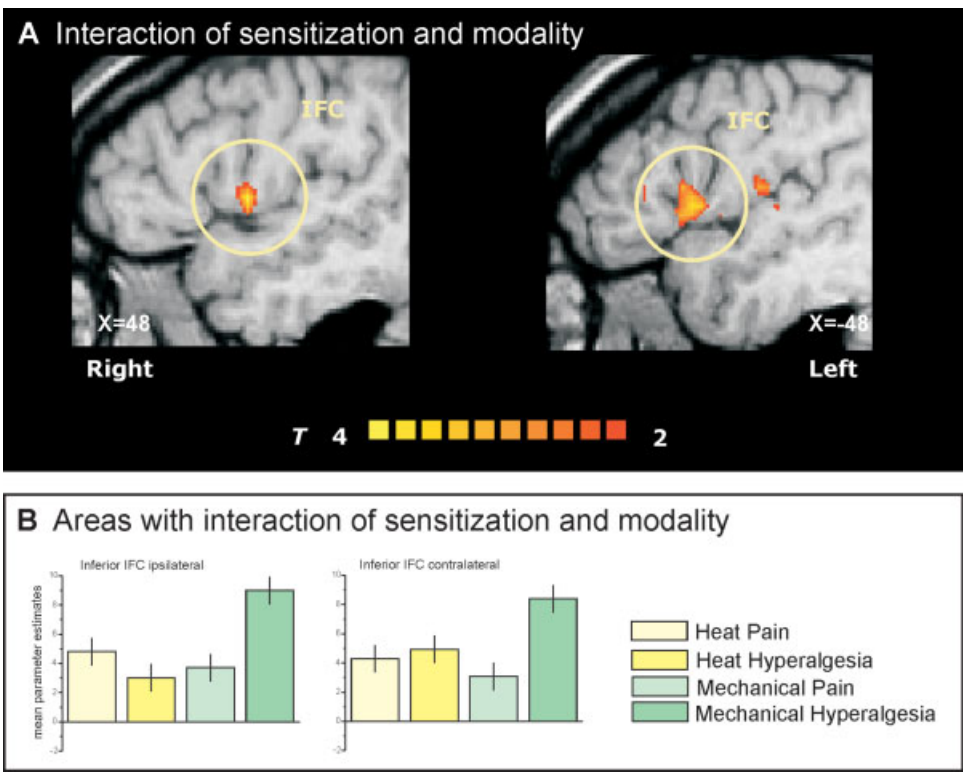

Figure 5.

[Baron et al. 1999; Ducreux et al., 2006; Lorenz et al., 2002; Maihofner and Handwerker, 2005; Maihofner et al., 2003, 2004, 2005, 2006a; Schweinhardt et al., 2006; Zambreanu et al., 2005]. Only minor effect of sensitization was found in primary somatosensory cortex (S1) and no effect of sensitization was found in the secondary somatosensory cortex (S2). Interestingly, a conjunction analysis of the effect of sensitization across both types of hyperalgesia revealed a common, for both modalities identical increase in activity only in the ACC, the bilateral anterior insula and parts of the bilateral IFC. All three regions are known to be involved in cognitive-emotional evaluation of pain. This shift from areas involved in sensory-discriminative processing to areas with a pivotal role in affective-motivational evaluation in the presence of a pathological painful state can be interpreted as an adaptation on the biological needs: the evaluation of the biological meaning of the pain gains more importance than spatial and intensity coding.

The anterior cingulated gyrus (ACC) has an important role in processing the affective-motivational component of pain [Apkarian et al., 2005; Sewards and Sewards, 2002; Vogt, 2005; Vogt and Sikes, 2000]. According to Vogt [2005] the cingulate gyrus can be divided into an anterior subgenual part (sACC) and an anterior perigenual part (pACC), the midcingulate cortex (MCC), and the posterior cingulated cortex (PCC). Other authors refer the MCC as the posterior ACC [Buchel et al., 2002; Maihofner and Handwerker, 2005; Mohr et al., 2005]. In our study, prominent activation was found in the posterior ACC (mainly BA 24 and, to lesser extend BA 32), a region activated constantly in pain-imaging studies [Apkarian et al., 2005]. Although there is evidence for pain-intensity coding in the posterior ACC [Mohr et al., 2005; Tolle et al., 1999], its most important role seems to be the cognitive and affective evaluation of nociceptive input [Apkarian et al., 2005; Buchel et al., 2002; Mohr et al., 2005; Tolle et al., 1999]. Hypnotic suggestions which altered the subjective affective component of painful stimuli also increased or decreased activation of ACC [Faymonville et al., 2000; Rainville et al., 1997, 1999]. During distraction tasks the cingulo-frontal cortex exerts top-down modulation of the PAG and posterior thalamus [Valet et al., 2004]. The region is activated during anticipation of pain [Hsieh et al., 1999] and during expectation of pain [Sawamoto et al., 2000]. Activity within posterior ACC (also known as the midcingulate region) (BA 24, "the sensory part") was found to be decreased during distraction from painful stimuli, whereas activity in perigenual cingulate (BA 32, "the cognitive part") was increased [Bantick et al., 2002; Frankenstein et al., 2001; Valet et al., 2004]. Furthermore, negative emotional context amplified pain-related responses of the ACC [Phillips et al., 2003; Ploghaus et al., 2001] and empathy for pain of others activates the rostral ACC (Singer et al., 2004]. The anterior cingulate area that was found to be activated similarly during thermal and mechanical hyperalgesia as revealed by conjunction analysis in the present study, was also the posterior ACC, i.e., mainly Brodmann area 24 according to Vogt and colleagues [Vogt and Sikes, 2000; Vogt et al., 1995, 1996, 2005]. The PCC has recently been reported to be activated during mechanical hyperalgesia [Zambreanu et al., 2005] and by selective activation of mechano-insensitive c-nociceptors, which play a crucial

Figure 4.

Main effects of the factors "sensitization" and "modality". The *T*-statistic contrast maps show (**A**) the main effect of sensitization, averaged across both modalities, and (**B**) the main effect of modality, averaged across both sensitization states. Areas that are coded red/yellow in (A) showed a significantly greater response during the sensitized state compared with the nonsensitized state. Areas that are coded in red/yellow in (B) showed a significantly greater response to heat stimuli than to mechanical stimuli. Areas that are coded in blue/green in (B) showed a significantly greater response to mechanical stimuli than to heat stimuli. The group statistic contrast maps are registered onto a Talairach-transformed brain, thresholded at $T > 2$, $P < 0.05$ uncorrected for multiple comparisons and a cluster threshold of 300 voxels. Activations seen in the left hemisphere are contralateral to the stimulation side. The Talairach-coordinates, *T*-scores, Bonferroni-corrected *P* values and cluster sizes are depicted in Table I. Abbreviations: ACC, anterior cingulate cortex; PCC, posterior cingulate cortex; TH, thalamus; SFC, superior frontal cortex; MFC, middle frontal cortex; IFC, inferior frontal cortex; S1, primary somatosensory cortex; S2, secondary somatosensory cortex; PA, parietal association cortex. The mean parameter estimates (beta values) for each condition in (**C**) areas with a main effect of sensitization, (**D**) areas with a main effect of modality, and (**E**) areas with a main effect of sensitization and modality are shown. Error bars indicate SEM.

Figure 5.

Interaction contrast. The (**A**) *T*-statistic contrast map shows interaction of the factors "sensitization" and "modality" only located bilaterally at the caudal part of inferior frontal cortex (IFC). The (**B**) mean parameter estimates of the four conditions reveal the nature of sensitization–modality interaction: only mechanical stimuli on sensitized skin lead to increased activation in this subregion of the IFC. The group statistic contrast maps are registered onto a Talairach-transformed brain, thresholded at $T > 2$, $P < 0.05$ uncorrected for multiple comparisons and a cluster threshold of 300 voxels. Activations seen in the left hemisphere are contralateral to the stimulation side. The Talairach-coordinates and cluster sizes are depicted in Table I.

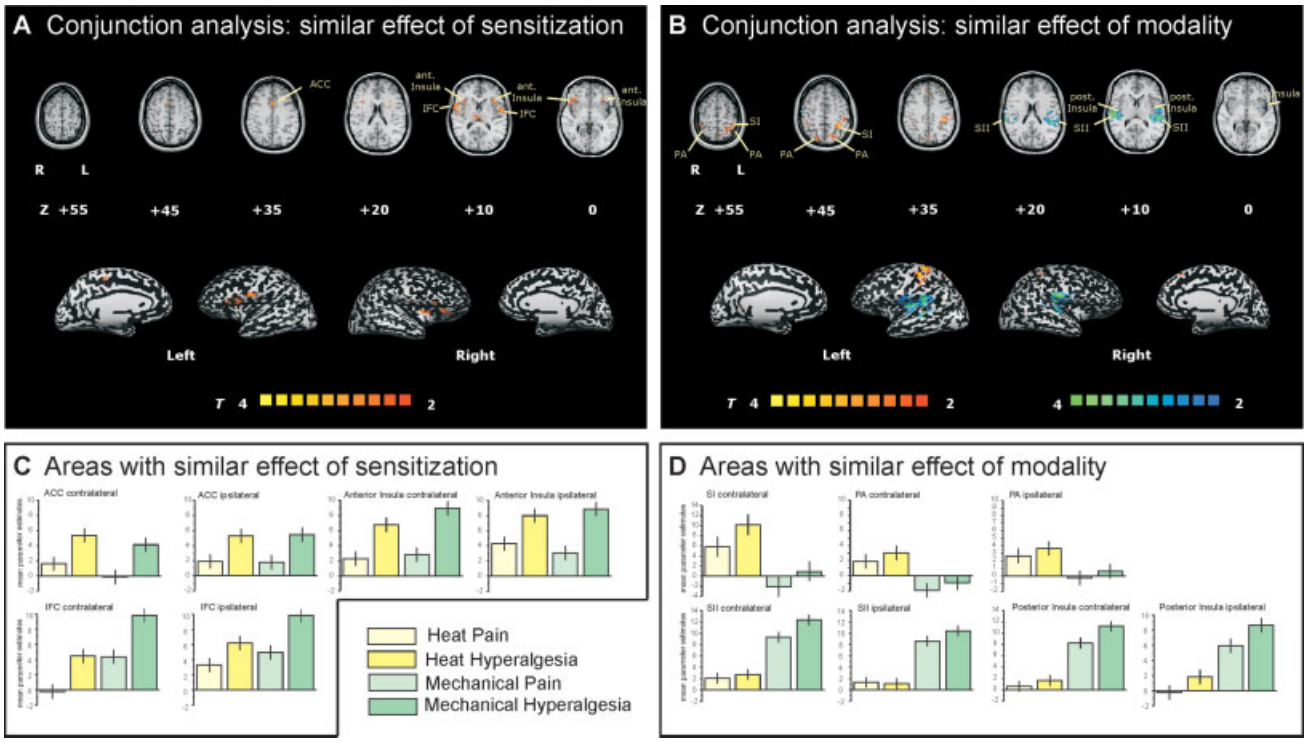

Figure 6.

Common activation patterns: Conjunction analysis reveals areas with (**A**) similar effect of sensitization regardless of modality and (**B**) similar effect of modality regardless of sensitization state. Areas that are coded red/yellow in (A) showed a similar effect of sensitization during heat and mechanical stimuli. Areas that are coded in red/yellow in (B) showed a similar response to heat stimuli in the nonsensitized and the sensitized area. Areas that are coded in blue/green in (B) showed a similar response to mechanical stimuli in the nonsensitized and the sensitized area. The group statistic contrast maps are registered onto a Talairach-transformed brain, thresholded at $T > 2$, $P < 0.05$ uncorrected for multiple comparisons and a cluster threshold of 300 voxels. Activations seen in the left hemisphere are contralateral to the stimulation side. The Talairach-coordinates and cluster sizes are depicted in Table I. Abbreviations: ACC, anterior cingulate cortex; PCC, posterior cingulate cortex; TH, thalamus; SFC, superior frontal cortex; MFC, middle frontal cortex; IFC, inferior frontal cortex; S1, primary somatosensory cortex; S2, secondary somatosensory cortex; PA, parietal association cortex. The mean parameter estimates (beta values) for each condition in (**C**) areas with a common effect of sensitization and (**D**) areas with a common effect of modality are shown. Error bars indicate SEM.

role in inflammatory pain, but not by stimulation of polymodal c-nocicepors [Ruehle et al., 2006]. Therefore, the PCC seems to play an important role in the processing of hyperalgesia. This is also in line with our present results, as the PCC showed strong activations during both hyperalgesia conditions.

The insular cortex is a multidimensional integration site for pain [Brooks and Tracey, 2007; Craig and Bushnell, 1994; Craig et al., 1996, 2000]. It has direct input from the thalamus, thus is connected to the lamina I spinothalamic pathway, and has output to PFC, striatum, and PA [Craig, 2003c]. Its important role in pain processing is mirrored by somatotopic arrangement [Brooks et al., 2005; Hua le et al., 2005]. In particular, the caudal anterior part has been reported to have pain intensity coding abilities, whereas the rostral anterior part seems to be involved in nociceptive processing during pathological pain states [Schweinhardt et al., 2006]. Moreover, the anterior part of the insula is shown to play a crucial role in interoception and homeostasis [Craig, 2002, 2003a,b] and is important for afferent autonomic integration and emotions [Craig, 2005].

We found a prominent sensitization-related increase in activation during both modalities in PFC with the most prominent increase in the DLPFC. Interestingly, the bilateral caudal part of the IFC was the only region with a significant interaction of sensitization and modality. Several previous functional imaging studies demonstrated PFC activity during experimental [Baron et al., 1999; Iadarola et al., 1998; Maihofner and Handwerker, 2005; Witting et al., 2001] or clinical forms of hyperalgesia [Ducreux et al., 2006; Maihofner et al., 2005]. In a previous study done by our group, stronger activations of GC, contralateral MFC (BA 9), and anterior insula by primary (heat-) compared with secondary (mechanical-) hyperalgesia cor-

related to higher ratings of the stimulus-related unpleasantness [Maihofner and Handwerker, 2005]. A PET study comparing heat allodynia to normal heat pain [Lorenz et al., 2002] found increased activation of a medial thalamic pathway to frontal cortices during the allodynia condition, exemplified as a shift toward the medial pain system including the frontal cortex and GC. Numerous studies have demonstrated the crucial role for the PFC for psychological modulation of pain. The PFC (especially MFC and ACC) was activated during anticipation of pain [Hsieh et al., 1999; Ploghaus et al., 1999]. Pain-evoked activity increased mainly in orbitofrontal cortices during distraction from pain when performing a cognitive task [Bantick et al., 2002; Petrovic et al., 2000]. Furthermore, the PFC (SFC) was activated during expectation of pain [Ploghaus et al., 2000]. Also, attention to painful stimuli resulted in increased DLPFC activity [Peyron et al., 1999]. Particularly, the DLPFC seems to exert active control on pain perception by modulating corticosubcortical and corticocortical pathways [Lorenz et al., 2003]. The modulatory function of the PFC on nociceptive processing has also been demonstrated by its prominent role in the placebo effect. Placebo analgesia was associated with increased activity during anticipation of pain in the dorsolateral prefrontal and orbitofrontal cortex, but was related to decreased brain activity in pain-sensitive brain regions, including the thalamus, insula, and ACC [Wager et al., 2004]. Interaction between stimulus modality and sensitization state was found in the bilateral caudal part of the IFC. The IFC is regularly activated in pain-imaging studies. However, its functional relevance is largely unknown. Interestingly, this region was recently reported to be pivotally involved in imitation of facial emotional expression [Lee et al., 2006]. We did not measure facial grimacing during the two pain modalities, so we cannot exclude a contribution of this factor to the observed difference. Altogether, there seems to be a global role for the PFC in the regulation of inhibition and excitation in distributed neural networks. It is suggested that the PFC exerts an inhibitory control of noxious input and thus represents one of the central structures for pain modulation.

Differential Processing of Stimulus Modality

Factor analysis further revealed that the main difference between heat and mechanical hyperalgesia is a differential processing of thermal and mechanical pain per se. Heat hyperalgesia, i.e., comparison of brain activations during thermal stimulation inside and outside the area of UV-application, led to activations of primary and secondary somatosensory cortices (S1 and S2), associative-somatosensory cortices (PA), insula, cingulate cortex (ACC), and PFC (SFC, MFC, IFC). In direct *T*-statistical comparison of heat vs. mechanical hyperalgesia, heat hyperalgesia activated to significantly greater extent the anterior insula, PA, PFC (SFC, MFC and IFC), and anterior cingulate gyrus (ACC), the latter both attributed to the medial pain system. One possible factor accounting for that difference aside the modality could be the different dynamic aspects of the stimuli: heat pain was applied tonic, mechanical pain phasic. It has been shown that the aversive component is greater for tonic pain than for phasic pain [Chen and Treede, 1985). This would fit to the increased frontal activations during heat hyperalgesia compared with mechanical hyperalgesia. Another contributing factor could be a stronger activation of the descending inhibitory control system due to the tonic character of the heat stimuli. Especially, the DLPFC, which was activated more during heat stimuli in our study was reported to play a pivotal role in descending pain modulation [Lorenz et al., 2003]. Also the spatial extend of the stimuli may contribute to the modality differences observed. It was shown that larger areas of pain application resulted in increased fMRI responses in S1 [Apkarian et al., 2000]. Moreover, heat hyperalgesia led to significant stronger activation in bilateral parietal cortex (PA). This area belongs to associative-somatosensory cortices and has a role as somatosensory integration center for spatial information and environmental processes. Its involvement in pain processing has been documented several times in both experimental [Maihofner et al., 2004; Witting et al., 2001] and neuropathic pain [Hsieh et al., 1995; Maihofner et al., 2005]. It may be hypothesized that activation during hyperalgesic states reflects higher sensory integration processes and that this region is involved in directing attention to and processing of painful stimuli.

Mechanical hyperalgesia, thus comparison of brain activations during mechanical impact stimulation inside and outside the area of UV application showed significantly more activation of secondary somatosensory cortices (S2), anterior and posterior insula, PFC, ACC, PA, PCC, basal ganglia, and thalamus. This pattern of activation is consistent with previous literature investigating brain activation during mechanical hyperalgesia [Baron et al., 1999; Iadarola et al., 1998; Maihofner and Handwerker, 2005; Maihofner et al., 2004; Witting et al., 2001; Zambreanu et al., 2005] despite the use of different methods for the induction of hyperalgesia. When compared with heat hyperalgesia, mechanical hyperalgesia led to an increased activation of secondary somatosensory cortex (S2) and posterior insular cortex. The lateral pain system consists of primary (S1) and secondary (S2) somatosensory cortices. It encodes the sensory-discriminative component of pain. S2 responses to thermal laser stimuli encoded gradually the intensity of stimuli from sensory threshold up to a level next to pain threshold but showed a ceiling effect for higher painful intensities [Frot et al., 2007]. The significant dominance of mechanical stimuli in S2 activation may be attributed to spatial encoding of the exact pain location to plan withdrawal. It is possible that increased S2 activation is due to an attentional drive toward the mechanical stimulus, given that attentional processes can significantly influence somatosensory response [Johansen-Berg et al., 2000]. Aside from modality, the difference might be also a result of the phasic character of the mechanical impact stimulation, espe-

cially in consideration of a previously described S2 ceiling effect to graded painful stimuli [Frot et al., 2007].

The posterior insular cortex was also more strongly activated during mechanical hyperalgesia. This cortical region encodes the intensity [Coghill et al., 1999; Craig et al., 2000], the laterality [Brooks et al., 2002], and the somatotopy [Brooks et al., 2005] of nociceptive stimuli. This area seems to be more involved in the triggering of affective recognition of, and motor reaction to, noxious stimuli, whereas S2 would be more dedicated to finer-grain discrimination of stimulus intensity, from nonpainful to painful levels [Frot et al., 2007].

In summary, in the present study we found that different types of hyperalgesia produce different brain activation patterns. We found a dominance of prefrontal and cingulate cortex activity during heat hyperalgesia and a dominance of S2 and posterior insula during mechanical hyperalgesia at weighted pain intensities. The basis of the differences was the differential processing of thermal and mechanical pain, and, to a minor extent, an interaction of sensitization and modality in the caudal portion of the IFC. Moreover, the data give evidence for the existence of a common "sensitization network" consisting of ACC, bilateral anterior insula and parts of the IFC.

ACKNOWLEDGMENTS

We thank Gabi Göhring-Waldeck for excellent technical assistance. We are indebted to Dr. Richard Carr and anonymous reviewers for useful comments on the manuscript.

REFERENCES

Apkarian AV, Gelnar PA, Krauss BR, Szeverenyi NM (2000): Cortical responses to thermal pain depend on stimulus size: A functional MRI study. J Neurophysiol 83:3113–3122.

Apkarian AV, Bushnell MC, Treede RD, Zubieta JK (2005): Human brain mechanisms of pain perception and regulation in health and disease. Eur J Pain 9:463–484.

Bantick SJ, Wise RG, Ploghaus A, Clare S, Smith SM, Tracey I (2002): Imaging how attention modulates pain in humans using functional MRI. Brain 125(Pt 2):310–319.

Baron R, Baron Y, Disbrow E, Roberts TP (1999): Brain processing of capsaicin-induced secondary hyperalgesia: A functional MRI study. Neurology 53:548–557.

Bickel A, Dorfs S, Schmelz M, Forster C, Uhl W, Handwerker HO(1998): Effects of antihyperalgesic drugs on experimentally induced hyperalgesia in man. Pain 76:317–325.

Brooks JC, Tracey I (2007): The insula: A multidimensional integration site for pain. Pain 128:1–2.

Brooks JC, Nurmikko TJ, Bimson WE, Singh KD, Roberts N (2002): fMRI of thermal pain: Effects of stimulus laterality and attention. Neuroimage 15:293–301.

Brooks JC, Zambreanu L, Godinez A, Craig AD, Tracey I (2005): Somatotopic organisation of the human insula to painful heat studied with high resolution functional imaging. Neuroimage 27:201–209.

Buchel C, Bornhovd K, Quante M, Glauche V, Bromm B, Weiller C (2002): Dissociable neural responses related to pain intensity, stimulus intensity, and stimulus awareness within the anterior cingulate cortex: A parametric single-trial laser functional magnetic resonance imaging study. J Neurosci 22:970–976.

Chen AC, Treede RD (1985): The McGill Pain Questionnaire in the assessment of phasic and tonic experimental pain: Behavioral evaluation of the 'pain inhibiting pain' effect. Pain 22:67–79.

Coghill RC, Sang CN, Maisog JM, Iadarola MJ (1999): Pain intensity processing within the human brain: A bilateral, distributed mechanism. J Neurophysiol 82:1934–1943.

Craig AD (2002): How do you feel? Interoception: The sense of the physiological condition of the body. Nat Rev Neurosci 3:655–666.

Craig AD (2003a): Interoception: The sense of the physiological condition of the body. Curr Opin Neurobiol 13:500–505.

Craig AD (2003b): A new view of pain as a homeostatic emotion. Trends Neurosci 26:303–307.

Craig AD (2003c): Pain mechanisms: Labeled lines versus convergence in central processing. Annu Rev Neurosci 26:1–30.

Craig AD (2005): Forebrain emotional asymmetry: A neuroanatomical basis? Trends Cogn Sci 9:566–571.

Craig AD, Bushnell MC (1994): The thermal grill illusion: Unmasking the burn of cold pain. Science 265:252–255.

Craig AD, Reiman EM, Evans A, Bushnell MC (1996): Functional imaging of an illusion of pain. Nature 384:258–260.

Craig AD, Chen K, Bandy D, Reiman EM (2000): Thermosensory activation of insular cortex. Nat Neurosci 3:184–190.

Ducreux D, Attal N, Parker F, Bouhassira D (2006): Mechanisms of central neuropathic pain: A combined psychophysical and fMRI study in syringomyelia. Brain 129(Pt 4):963–976.

Faymonville ME, Laureys S, Degueldre C, DelFiore G, Luxen A, Franck G, Lamy M, Maquet P (2000): Neural mechanisms of antinociceptive effects of hypnosis. Anesthesiology 92:1257–1267.

Frankenstein UN, Richter W, McIntyre MC, Remy F (2001): Distraction modulates anterior cingulate gyrus activations during the cold pressor test. Neuroimage 14:827–836.

Frot M, Magnin M, Mauguiere F, Garcia-Larrea L (2007): Human SII and posterior insula differently encode thermal laser stimuli. Cereb Cortex 17:610–620.

Harrison GI, Young AR, McMahon SB (2004): Ultraviolet radiation-induced inflammation as a model for cutaneous hyperalgesia. J Invest Dermatol 122:183–189.

Hofbauer RK, Rainville P, Duncan GH, Bushnell MC (2001): Cortical representation of the sensory dimension of pain. J Neurophysiol 86:402–411.

Hoffmann RT, Schmelz M (1999): Time course of UVA- and UVB-induced inflammation and hyperalgesia in human skin. Eur J Pain 3:131–139.

Hsieh JC, Belfrage M, Stone-Elander S, Hansson P, Ingvar M (1995): Central representation of chronic ongoing neuropathic pain studied by positron emission tomography. Pain 63:225–236.

Hsieh JC, Stone-Elander S, Ingvar M (1999): Anticipatory coping of pain expressed in the human anterior cingulate cortex: A positron emission tomography study. Neurosci Lett 262:61–64.

Hua le H, Strigo IA, Baxter LC, Johnson SC, Craig AD (2005): Anteroposterior somatotopy of innocuous cooling activation focus in human dorsal posterior insular cortex. Am J Physiol Regul Integr Comp Physiol 289:R319–R325.

Iadarola MJ, Berman KF, Zeffiro TA, Byas-Smith MG, Gracely RH, Max MB, Bennett GJ (1998): Neural activation during acute capsaicin-evoked pain and allodynia assessed with PET. Brain 121(Pt 5):931–947.

Jensen TS, Baron R (2003): Translation of symptoms and signs into mechanisms in neuropathic pain. Pain 102:1–8.

Johansen-Berg H, Christensen V, Woolrich M, Matthews PM (2000): Attention to touch modulates activity in both primary and secondary somatosensory areas. Neuroreport 11:1237–1241.

Klein T, Magerl W, Rolke R, Treede RD (2005): Human surrogate models of neuropathic pain. Pain 115:227–233.

Kohlloffel LU, Koltzenburg M, Handwerker HO (1991): A novel technique for the evaluation of mechanical pain and hyperalgesia. Pain 46:81–87.

Koppert W, Brueckl V, Weidner C, Schmelz M (2004): Mechanically induced axon reflex and hyperalgesia in human UV-B burn are reduced by systemic lidocaine. Eur J Pain 8:237–244.

Lee TW, Josephs O, Dolan RJ, Critchley HD (2006): Imitating expressions: Emotion-specific neural substrates in facial mimicry. Soc Cogn Affect Neurosci 1:122–135.

Lorenz J, Cross D, Minoshima S, Morrow T, Paulson P, Casey K (2002): A unique representation of heat allodynia in the human brain. Neuron 35:383–393.

Lorenz J, Minoshima S, Casey KL (2003): Keeping pain out of mind: The role of the dorsolateral prefrontal cortex in pain modulation. Brain 126(Pt 5):1079–1091.

Maihofner C, Handwerker HO (2005): Differential coding of hyperalgesia in the human brain: A functional MRI study. Neuroimage 28:996–1006.

Maihofner C, Neundorfer B, Stefan H, Handwerker HO (2003): Cortical processing of brush-evoked allodynia. Neuroreport 14:785–789.

Maihofner C, Schmelz M, Forster C, Neundorfer B, Handwerker HO (2004): Neural activation during experimental allodynia: A functional magnetic resonance imaging study. Eur J Neurosci 19:3211–3218.

Maihofner C, Forster C, Birklein F, Neundorfer B, Handwerker HO (2005): Brain processing during mechanical hyperalgesia in complex regional pain syndrome: A functional MRI study. Pain 114:93–103.

Maihofner C, Handwerker HO, Birklein F (2006a): Functional imaging of allodynia in complex regional pain syndrome. Neurology 66:711–717.

Maihofner C, Herzner B, Otto Handwerker H (2006b): Secondary somatosensory cortex is important for the sensory-discriminative dimension of pain: A functional MRI study. Eur J Neurosci 23:1377–1383.

Mailis-Gagnon A, Giannoylis I, Downar J, Kwan CL, Mikulis DJ, Crawley AP, Nicholson K, Davis KD (2003): Altered central somatosensory processing in chronic pain patients with "hysterical" anesthesia. Neurology 60:1501–1507.

Melzack R (1999): From the gate to the neuromatrix. Pain(Suppl 6):S121–S126.

Mohr C, Binkofski F, Erdmann C, Buchel C, Helmchen C (2005): The anterior cingulate cortex contains distinct areas dissociating external from self-administered painful stimulation: A parametric fMRI study. Pain 114:347–357.

Ochoa JL, Yarnitsky D (1993): Mechanical hyperalgesias in neuropathic pain patients: Dynamic and static subtypes. Ann Neurol 33:465–472.

Petrovic P, Ingvar M, Stone-Elander S, Petersson KM, Hansson P (1999): A PET activation study of dynamic mechanical allodynia in patients with mononeuropathy. Pain 83:459–470.

Petrovic P, Petersson KM, Ghatan PH, Stone-Elander S, Ingvar M (2000): Pain-related cerebral activation is altered by a distracting cognitive task. Pain 85:19–30.

Peyron R, Garcia-Larrea L, Gregoire MC, Costes N, Convers P, Lavenne F, Mauguiere F, Michel D, Laurent B (1999): Haemodynamic brain responses to acute pain in humans: Sensory and attentional networks. Brain 122(Pt 9):1765–1780.

Peyron R, Schneider F, Faillenot I, Convers P, Barral FG, Garcia-Larrea L, Laurent B (2004): An fMRI study of cortical representation of mechanical allodynia in patients with neuropathic pain. Neurology 63:1838–1846.

Phillips ML, Gregory LJ, Cullen S, Coen S, Ng V, Andrew C, Giampietro V, Bullmore E, Zelaya F, Amaro E and others (2003): The effect of negative emotional context on neural and behavioural responses to oesophageal stimulation. Brain 126(Pt 3): 669–684.

Ploghaus A, Tracey I, Gati JS, Clare S, Menon RS, Matthews PM, Rawlins JN (1999): Dissociating pain from its anticipation in the human brain. Science 284:1979–1981.

Ploghaus A, Tracey I, Clare S, Gati JS, Rawlins JN, Matthews PM (2000): Learning about pain: The neural substrate of the prediction error for aversive events. Proc Natl Acad Sci USA 97:9281–9286.

Ploghaus A, Narain C, Beckmann CF, Clare S, Bantick S, Wise R, Matthews PM, Rawlins JN, Tracey I (2001): Exacerbation of pain by anxiety is associated with activity in a hippocampal network. J Neurosci 21:9896–9903.

Rainville P, Duncan GH, Price DD, Carrier B, Bushnell MC (1997): Pain affect encoded in human anterior cingulate but not somatosensory cortex. Science 277:968–971.

Rainville P, Carrier B, Hofbauer RK, Bushnell MC, Duncan GH (1999): Dissociation of sensory and affective dimensions of pain using hypnotic modulation. Pain 82:159–171.

Ruehle BS, Handwerker HO, Lennerz JK, Ringler R, Forster C (2006): Brain activation during input from mechanoinsensitive versus polymodal C-nociceptors. J Neurosci 26:5492–5499.

Sawamoto N, Honda M, Okada T, Hanakawa T, Kanda M, Fukuyama H, Konishi J, Shibasaki H (2000): Expectation of pain enhances responses to nonpainful somatosensory stimulation in the anterior cingulate cortex and parietal operculum/posterior insula: An event-related functional magnetic resonance imaging study. J Neurosci 20:7438–7445.

Schmelz M, Schmidt R, Weidner C, Hilliges M, Torebjork HE, Handwerker HO (2003): Chemical response pattern of different classes of C-nociceptors to pruritogens and algogens. J Neurophysiol 89:2441–2448.

Schmidt R, Schmelz M, Forster C, Ringkamp M, Torebjork E, Handwerker H (1995): Novel classes of responsive and unresponsive C nociceptors in human skin. J Neurosci 15(Pt 1):333–341.

Schweinhardt P, Glynn C, Brooks J, McQuay H, Jack T, Chessell I, Bountra C, Tracey I (2006): An fMRI study of cerebral processing of brush-evoked allodynia in neuropathic pain patients. Neuroimage 32:256–265.

Sewards TV, Sewards MA (2002): The medial pain system: Neural representations of the motivational aspect of pain. Brain Res Bull 59:163–180.

Singer T, Seymour B, O'Doherty J, Kaube H, Dolan RJ, Frith CD (2004): Empathy for pain involves the affective but not sensory components of pain. Science 303:1157–1162.

Sycha T, Anzenhofer S, Lehr S, Schmetterer L, Chizh B, Eichler HG, Gustorff B (2005): Rofecoxib attenuates both primary and secondary inflammatory hyperalgesia: A randomized, double blinded, placebo controlled crossover trial in the UV-B pain model. Pain 113:316–322.

Szolcsanyi J (1987): Selective responsiveness of polymodal nociceptors of the rabbit ear to capsaicin, bradykinin and ultra-violet irradiation. J Physiol 388:9–23.

Talairach J, Tournoux P (1988): Co-Planar Stereotaxic Atlas of the Human Brain. New York: Thieme. pp 1–122.

Tolle TR, Kaufmann T, Siessmeier T, Lautenbacher S, Berthele A, Munz F, Zieglgansberger W, Willoch F, Schwaiger M, Conrad B and others (1999): Region-specific encoding of sensory and affective components of pain in the human brain: A positron emission tomography correlation analysis. Ann Neurol 45:40–47.

Tracey I (2005): Nociceptive processing in the human brain. Curr Opin Neurobiol 15:478–487.

Treede RD, Kenshalo DR, Gracely RH, Jones AK (1999): The cortical representation of pain. Pain 79:105–111.

Urban L, Perkins MN, Campbell E, Dray A (1993): Activity of deep dorsal horn neurons in the anaesthetized rat during hyperalgesia of the hindpaw induced by ultraviolet irradiation. Neuroscience 57:167–172.

Valet M, Sprenger T, Boecker H, Willoch F, Rummeny E, Conrad B, Erhard P, Tolle TR (2004): Distraction modulates connectivity of the cingulo-frontal cortex and the midbrain during pain—An fMRI analysis. Pain 109:399–408.

Vogt BA (2005): Pain and emotion interactions in subregions of the cingulate gyrus. Nat Rev Neurosci 6:533–544.

Vogt BA, Sikes RW (2000): The medial pain system, cingulate cortex, and parallel processing of nociceptive information. Prog Brain Res 122:223–235.

Vogt BA, Nimchinsky EA, Vogt LJ, Hof PR (1995): Human cingulate cortex: Surface features, flat maps, and cytoarchitecture. J Comp Neurol 359:490–506.

Vogt BA, Derbyshire S, Jones AK (1996): Pain processing in four regions of human cingulate cortex localized with co-registered PET and MR imaging. Eur J Neurosci 8:1461–1473.

Wager TD, Rilling JK, Smith EE, Sokolik A, Casey KL, Davidson RJ, Kosslyn SM, Rose RM, Cohen JD (2004): Placebo-induced changes in FMRI in the anticipation and experience of pain. Science 303:1162–1167.

Witting N, Kupers RC, Svensson P, Arendt-Nielsen L, Gjedde A, Jensen TS (2001): Experimental brush-evoked allodynia activates posterior parietal cortex. Neurology 57:1817–1824.

Witting N, Kupers RC, Svensson P, Jensen TS (2006): A PET activation study of brush-evoked allodynia in patients with nerve injury pain. Pain 120:145–154.

Woolf CJ, Mannion RJ (1999): Neuropathic pain: Aetiology, symptoms, mechanisms, and management. Lancet 353:1959–1964.

Zambreanu L, Wise RG, Brooks JC, Iannetti GD, Tracey I (2005): A role for the brainstem in central sensitisation in humans. Evidence from functional magnetic resonance imaging. Pain 114:397–407.

Ziegler EA, Magerl W, Meyer RA, Treede RD (1999): Secondary hyperalgesia to punctate mechanical stimuli. Central sensitization to A-fibre nociceptor input. Brain 122(Pt 12):2245–2257.